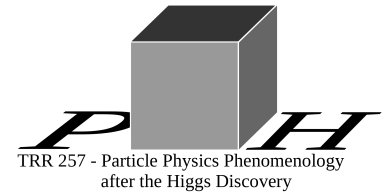


# Top quark mass at the LHC

M. Czakon

RWTH Aachen University



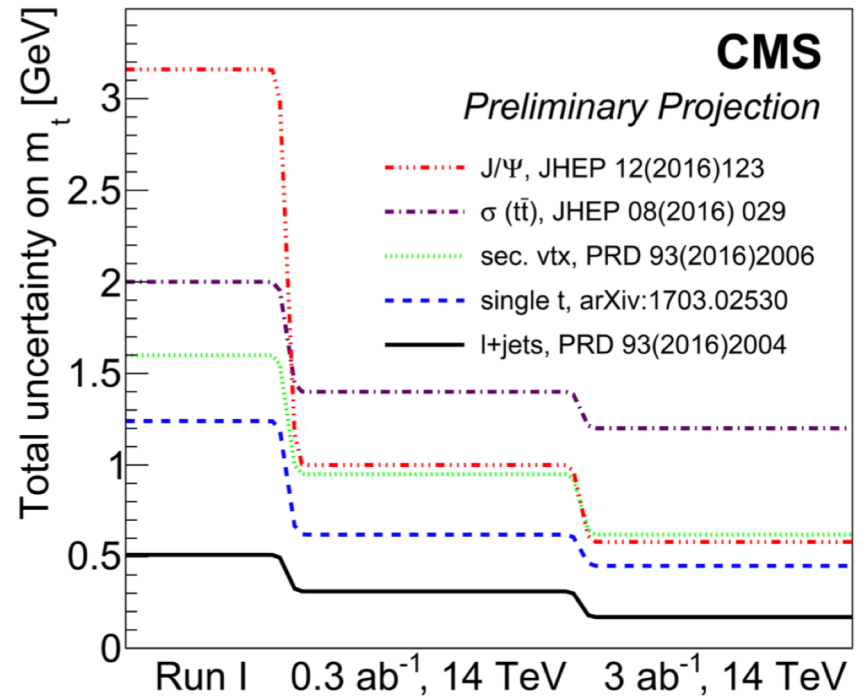
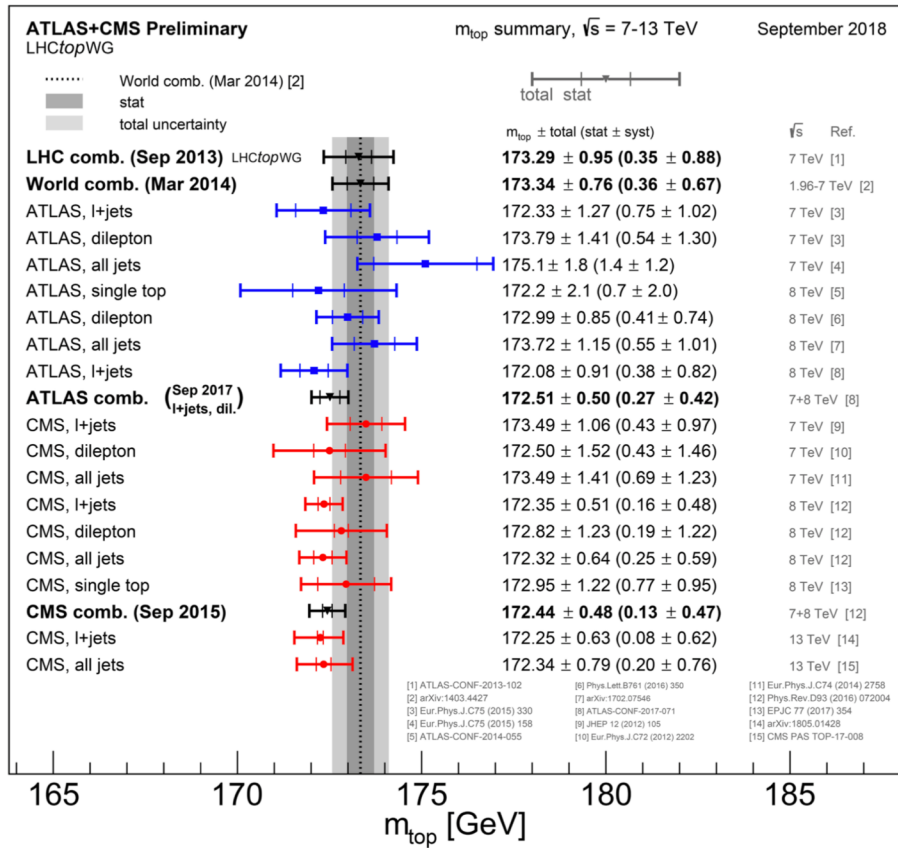
This talk is about issues surrounding the  
top-quark mass definition

The particular emphasis on some of the issues is  
due to performing the measurement at the LHC

This talk is for  
non-experts

The topic is  
controversial

# Status and prospects



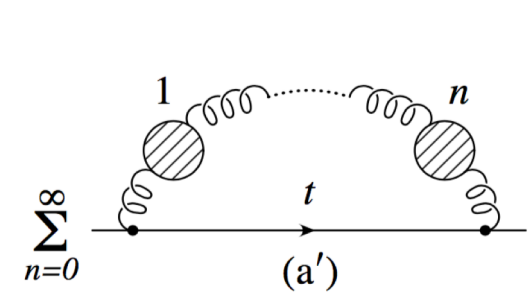
Why am **I**  
talking about this ?

(almost)  
every statement in physics  
is only approximate

- The Operator Product Expansion (used to decompose observables into non-perturbative and perturbative factors) **does not converge**
- The perturbative expansion of a partonic cross section **does not converge**
- The relation between the on-shell and short-distance masses of a quark **does not converge**

We are only optimizing asymptotic series

# Renormalons in the relation between on-shell and $\overline{\text{MS}}$ mass



$$m_{\text{pole}} = m_{\overline{\text{MS}}} + \mu C_F \frac{\alpha_S}{\pi} e^{-C/2} \sum_{n=0}^{\infty} 2^n n! (a_S b_0)^n$$

Bigi, Shifman, Uraltsev, Vainstein '94  
Beneke, Braun '94

Ambiguity estimate:  $1/\pi$  of imaginary part of Borel transform

$$\delta m = \mu 2C_F \frac{e^{-C/2}}{b_0} e^{-1/2 a_S b_0} \quad a_S(\mu^2) = \frac{1}{b_0 \ln \mu^2 / \Lambda_{\text{QCD}}^2}$$

$$\delta m = 2C_F \frac{e^{-C/2}}{b_0} \Lambda_{\text{QCD}}$$

Deeper understanding using renormalization group methods

Beneke '94

# Renormalons in the relation between on-shell and $\overline{\text{MS}}$ mass

Relation to  $\overline{\text{MS}}$  mass up to 4-loops

$$m_P = 163.643 + 7.557 + 1.617 + 0.501 + (0.195 \pm 0.005) \text{ GeV}$$

Beneke, Marquard, Nason, Steinhauser '16

Recent estimate of the ambiguity

$$\delta^{(5+)} m_P = 0.304_{-0.063}^{+0.012} (N) \pm 0.030 (m_{b,c}) \pm 0.009 (\alpha_s) \pm 0.108 (\text{ambiguity}) \text{ GeV}$$

...Countered with an estimate of ambiguity at 250 MeV

Hoang, Lepenik, Preisser '17

**This ambiguity is not the crux of the problem**

# A finite top-quark width does not solve the renormalon problem

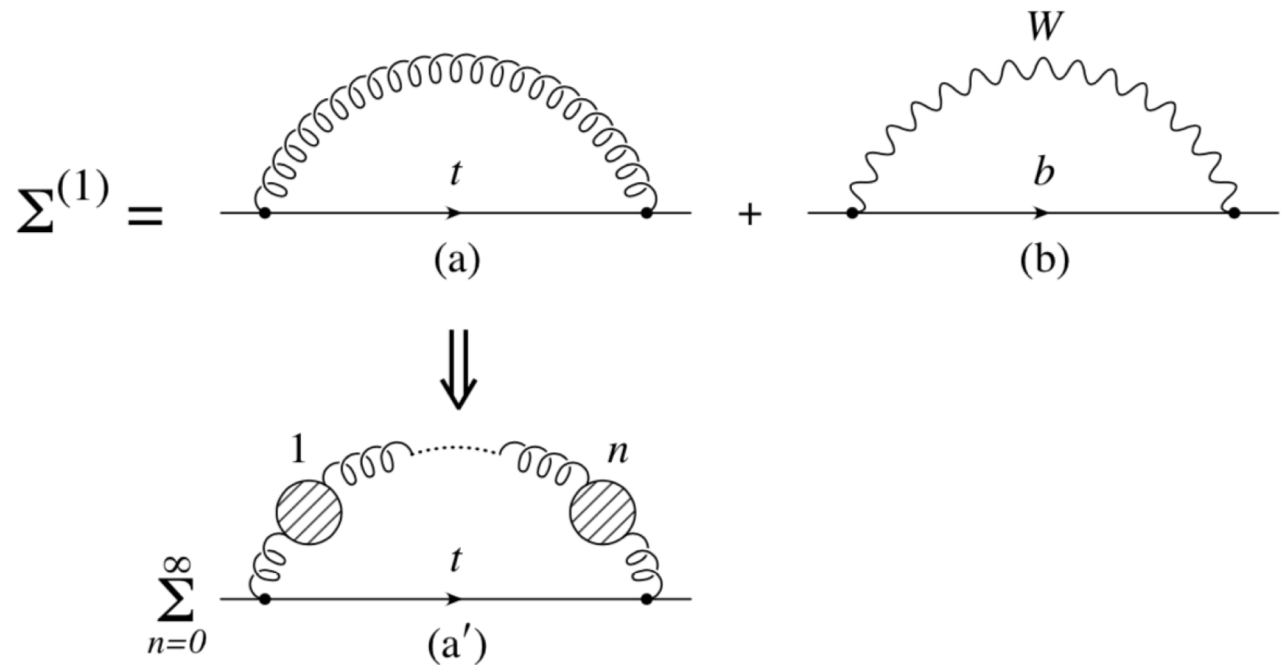


Figure 3: Diagrams contributing to the top-quark self-energy at leading order in  $\alpha_s$  and  $\alpha_W$ . Fig. (a') replaces Fig. (a) when summing to all orders in  $\beta_0\alpha_s$ .

# A finite top-quark width does not solve the renormalon problem

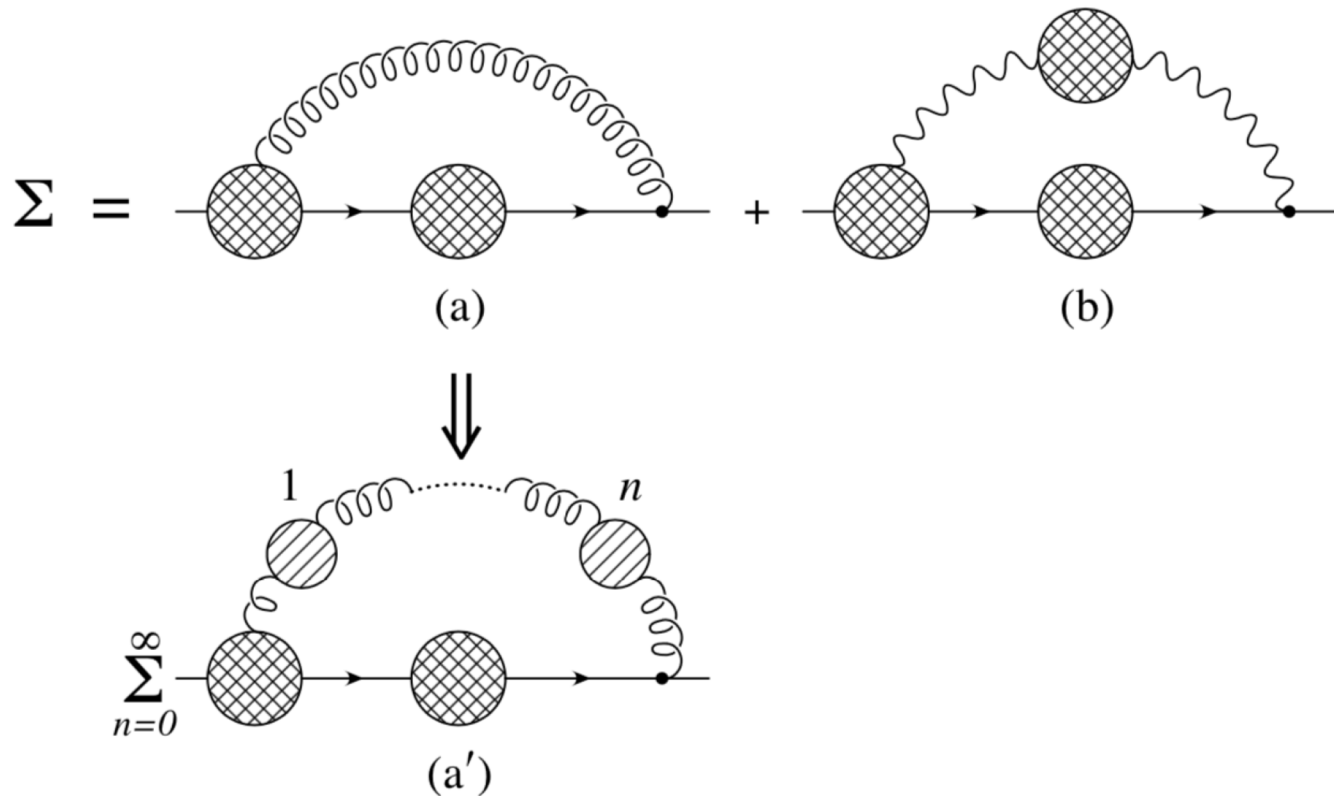


Figure 4: Diagrams contributing to the top-quark self energy at leading order in  $\alpha_s$ , but to all orders in  $\alpha_W$ . Fig. (a') replaces Fig. (a) when summing to all orders in  $\beta_0\alpha_s$ .

# A quark does not have a pole mass

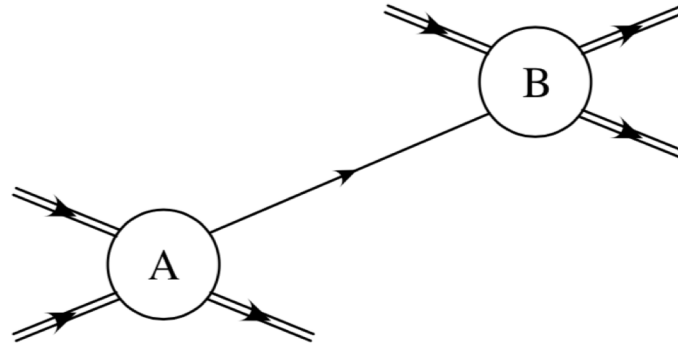


Figure 1: A scattering amplitude factorizes when an internal propagator is near its pole. The external lines represent color-singlet asymptotic states.

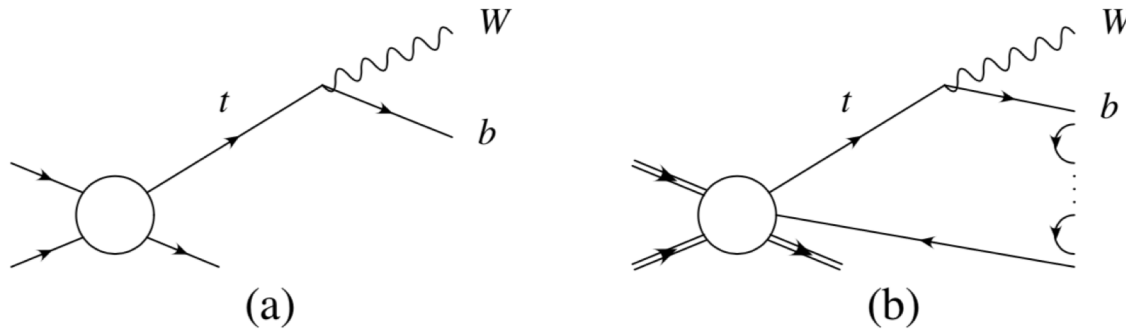


Figure 2: The production and decay of a top quark in (a) perturbation theory, and (b) nonperturbatively.

# No infrared region in definition of quark mass improves convergence

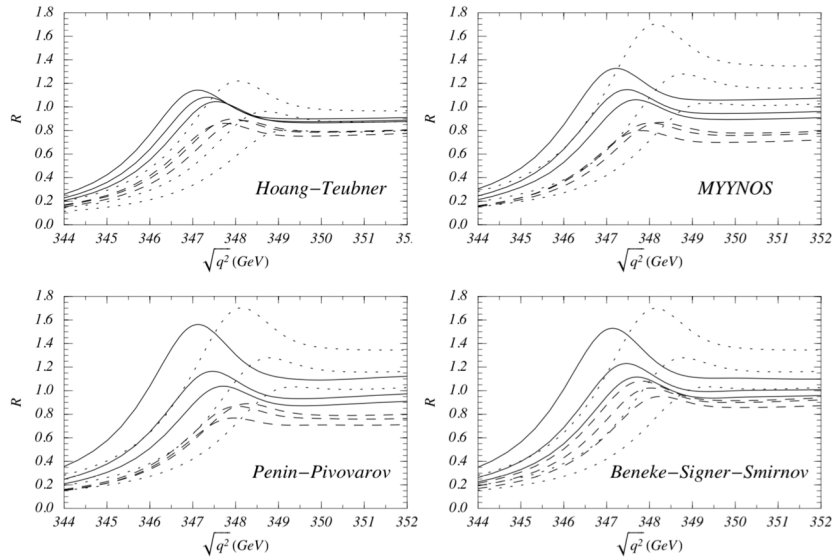


Figure 1: The total normalised photon-induced  $t\bar{t}$  cross section  $R$  at the LC versus the c.m. energy in the threshold regime at LO (dotted curves), NLO (dashed) and NNLO (solid) in the pole mass scheme for  $M_t^{\text{pole}} = 175.05$  GeV,  $\alpha_s(M_Z) = 0.119$ ,  $\Gamma_t = 1.43$  GeV and  $\mu_{\text{soft}} = 15, 30, 60$  GeV. The plots have been generated from results provided by the groups Hoang-Teubner (HT), Melnikov-Yelkhovsky-Yakovlev-Nagano-Ota-Sumino (MYYNOS), Penin-Pivovarov (PP) and Beneke-Signer-Smirnov (BSS).

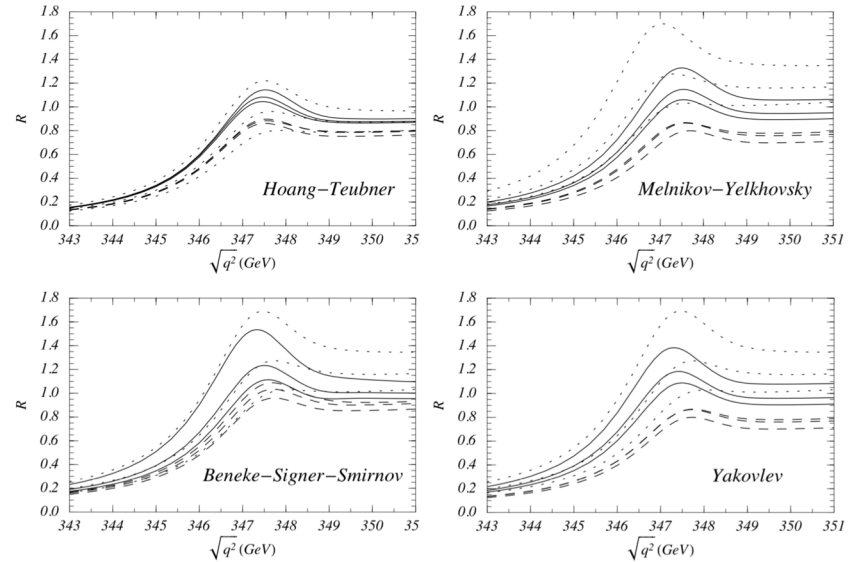


Figure 2: The total normalised photon-induced  $t\bar{t}$  cross section  $R$  at the LC versus the c.m. energy in the threshold regime at LO (dotted curves), NLO (dashed) and NNLO (solid). Hoang-Teubner used the 1S mass scheme with  $m_t^{1S} = 173.68$  GeV, Melnikov-Yelkhovsky the kinetic mass at 15 GeV with  $m_{t,15\text{GeV}}^{\text{kin}} = 173.10$  GeV, and Beneke-Signer-Smirnov and Yakovlev the PS mass at 20 GeV with  $m_{t,20\text{GeV}}^{\text{PS}} = 173.30$  GeV. The plots have been generated from results provided by the groups Hoang-Teubner (HT), Melnikov-Yelkhovsky (MY) and Beneke-Signer-Smirnov (BSS) and Yakovlev.

Hoang, Beneke, Melnikov, Nagano, Ota, Penin, Pivovarov, Signer, Smirnov, Sumino, Teubner, Yakovlev, Yelkhovsky '00

# The $\overline{\text{MS}}$ mass is not as universal as The $\overline{\text{MS}}$ strong coupling

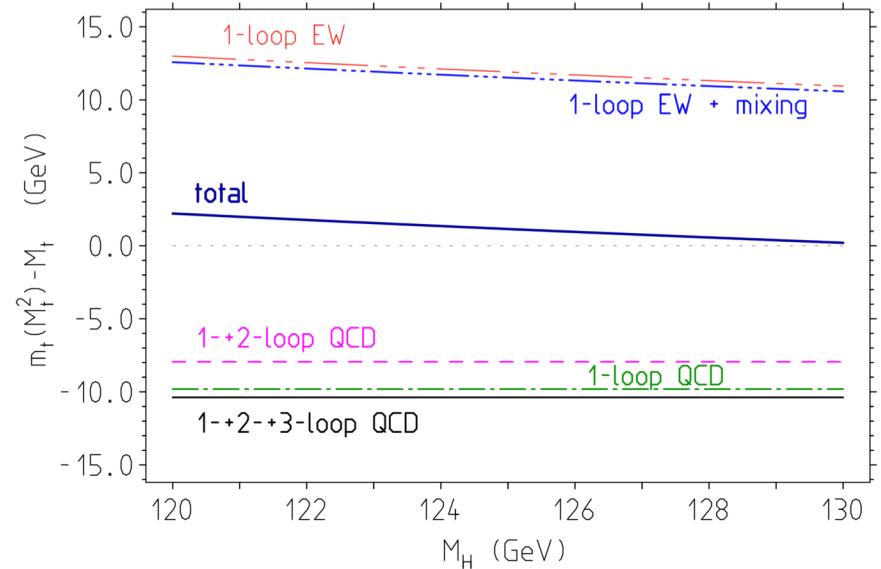
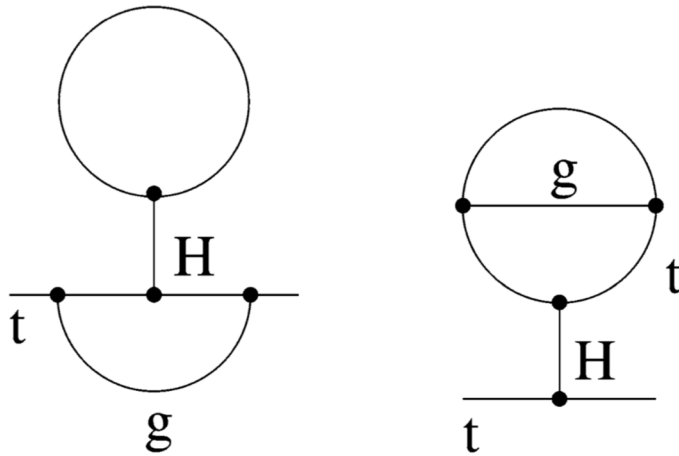


Table 1: The various contributions to  $m_t(M_t^2) - M_t$  in GeV.

$M_H$ [GeV]	$O(\alpha)$	$O(\alpha\alpha_s)$	$O(\alpha) + O(\alpha\alpha_s)$	$O(\alpha_s) + O(\alpha_s^2) + O(\alpha_s^3)$	total
124	12.11	-0.39	11.72	-10.38	1.34
125	11.91	-0.39	11.52	-10.38	1.14
126	11.71	-0.38	11.32	-10.38	0.94

# Renormalons are a proxy for non-perturbative effects

First discussed in the context of soft and collinear radiation for the thrust distribution in electron – positron collisions

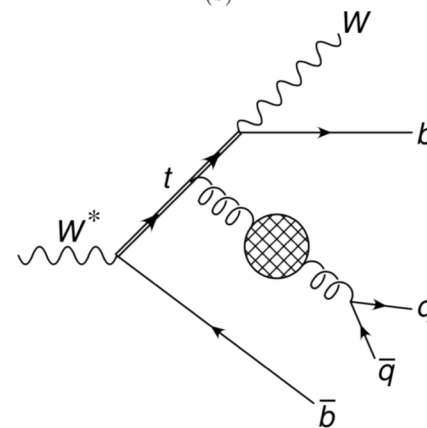
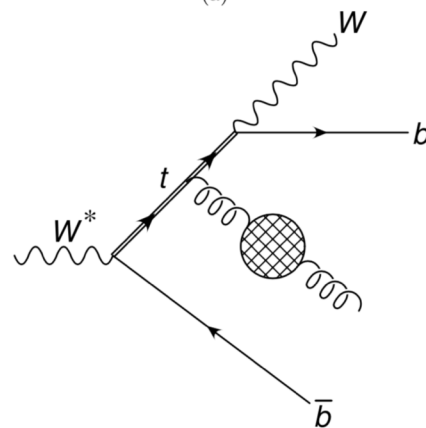
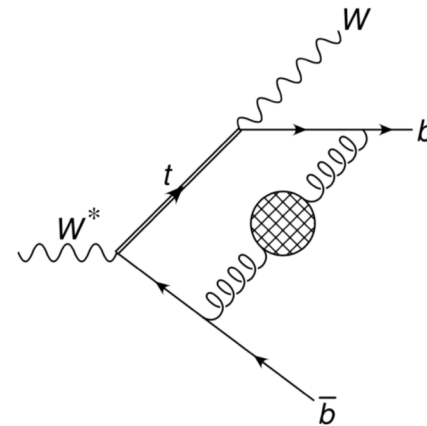
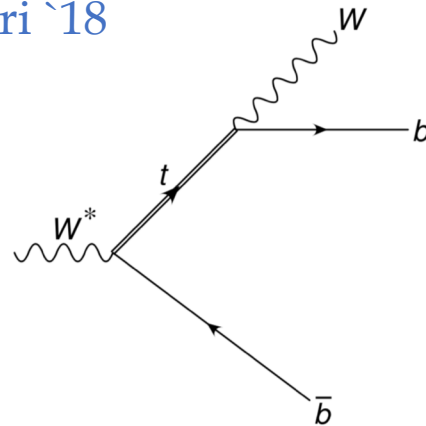
Gardi, Rathsman `01

and higher-twist contributions to deep inelastic scattering

Gardi, Roberts `02

# Renormalons are a proxy for non-perturbative effects

Recently revisited in  
Ravasio, Nason, Oleari '18



# Renormalons are a proxy for non-perturbative effects

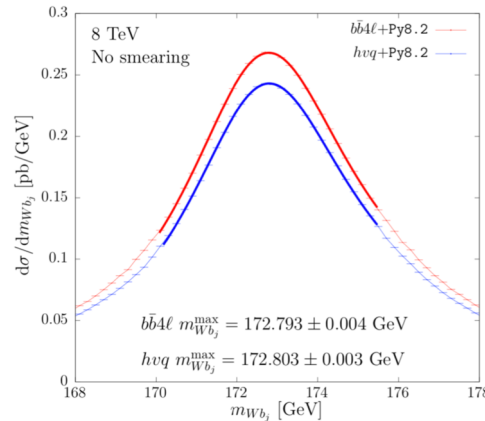
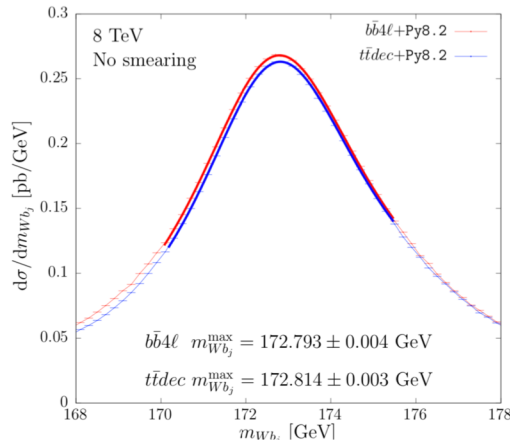
Recently revisited in

[Ravasio, Nason, Oleari '18](#)

1. total cross section: no infra-red sensitivity if the result is written in terms of short-distance masses; gets reflected in the convergence of perturbative series;
2. jet selection introduces linear infra-red sensitivity ( $1/R$ ) ; independent of the mass definition used; this is known and anticipated effect; the jet energy/momentum is affected by the hadronization in that way;
3. W-b invariant mass has linear infra-red sensitivity due to a final state jet, irrespective of the mass definition used;
4. Average energy of the W-boson: exhibits linear infra-red sensitivity in the narrow width limit, regardless of the mass used (boost to top rest frame); however, if the calculation is done keeping the width of the top quark, there is no linear infra-red sensitivity in case the short-distance mass is used.

# Modelling at hadron colliders

Parton showers matched after decay with NLO precision  
 Ravasio, Jezo, Nason, Oleari '18



hvq:  
 NLO production

tTdec:  
 NLO production and  
 decay, narrow width

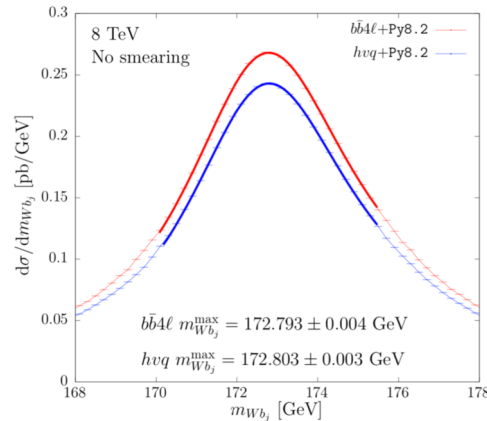
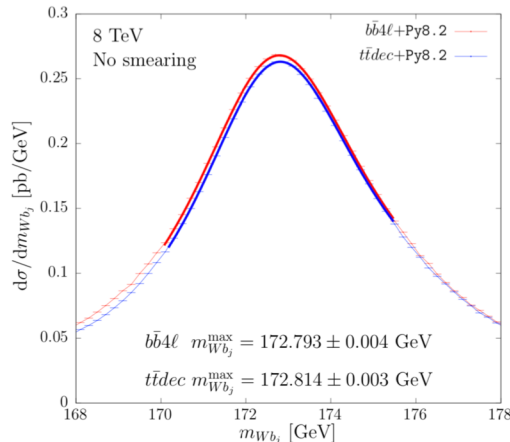
bB4l:  
 full NLO, off-shell

	PS only		full	
	No smearing	smearing	No smearing	smearing
$b\bar{b}4\ell$	172.522 GeV	171.403 GeV	172.793 GeV	172.717 GeV
$t\bar{t}dec - b\bar{b}4\ell$	$-18 \pm 2$ MeV	$+191 \pm 2$ MeV	$+21 \pm 6$ MeV	$+140 \pm 2$ MeV
$hvq - b\bar{b}4\ell$	$-24 \pm 2$ MeV	$-89 \pm 2$ MeV	$+10 \pm 6$ MeV	$-147 \pm 2$ MeV

Table 1: Differences in the  $m_{Wb_j}^{\max}$  for  $m_t=172.5$  GeV for  $t\bar{t}dec$  and  $hvq$  with respect to  $b\bar{b}4\ell$ , showered with `Pythia8.2`, at the NLO+PS level and at the full hadron level. Results obtained after smearing the  $m_{Wb_j}$  distribution with a Gaussian function with a 15 GeV width are also shown in order to mimic effects due to experimental uncertainties.

# Modelling at hadron colliders

Parton showers matched after decay with NLO precision  
 Ravasio, Jezo, Nason, Oleari '18



hvq:  
 NLO production

tTdec:  
 NLO production and  
 decay, narrow width

bB4l:  
 full NLO, off-shell

	No smearing		15 GeV smearing	
	He7.1	Py8.2 – He7.1	He7.1	Py8.2 – He7.1
$bb4l$	172.727 GeV	+66 ± 7 MeV	171.626 GeV	+1091 ± 2 MeV
$tTdec$	172.775 GeV	+39 ± 5 MeV	171.678 GeV	+1179 ± 2 MeV
$hvq$	173.038 GeV	-235 ± 5 MeV	172.319 GeV	+251 ± 2 MeV

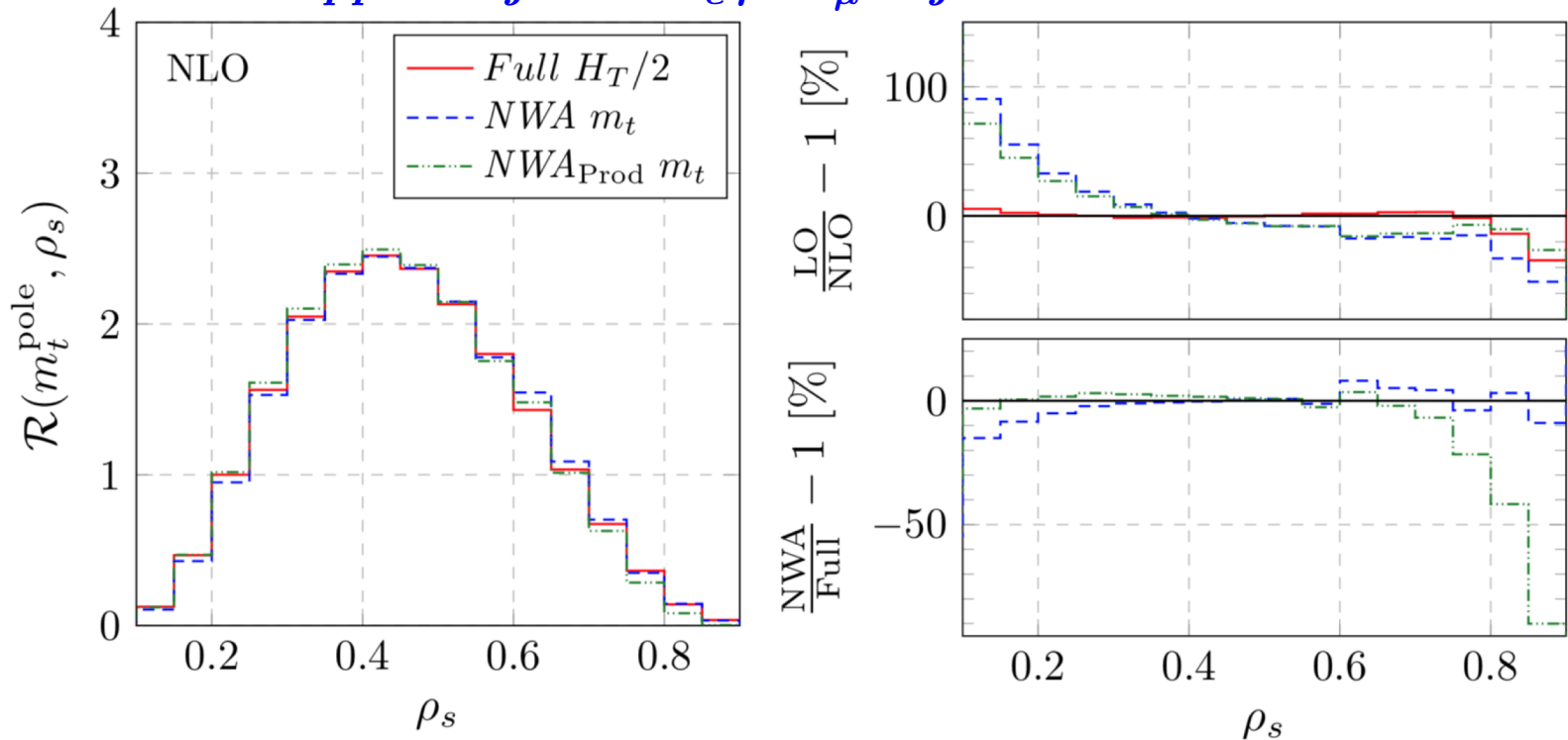
Table 2:  $m_{Wb_j}$  peak position for  $m_t=172.5$  GeV obtained with the three different generators, showered with Herwig7.1 (He7.1). The differences with Pythia8.2 (Py8.2) are also shown.

# Modelling at hadron colliders

Observable used for a recent top quark mass determination

Off-shell, NWA

$pp \rightarrow t\bar{t}j \rightarrow e^+ \nu_e \mu^- \bar{\nu}_\mu b\bar{b}j$  @ 13 TeV LHC



$$\mathcal{R}(m_t^{\text{pole}}, \rho_s) = \frac{1}{\sigma_{t\bar{t}j}} \frac{d\sigma_{t\bar{t}j}}{d\rho_s}(m_t^{\text{pole}}, \rho_s)$$

$$\rho_s = \frac{2m_0}{M_{t\bar{t}j}}$$

Alioli, Fernandez, Fuster, Irles, Moch, Uwer, Vos '13

# Modelling at hadron colliders

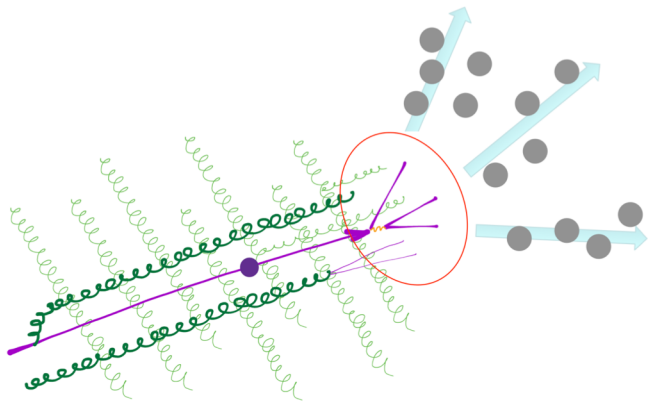
2.5 fb<sup>-1</sup>

$pp \rightarrow t\bar{t}j \rightarrow e^+ \nu_e \mu^- \bar{\nu}_\mu b\bar{b}j$  @ 13 TeV LHC

Theory, NLO QCD CT14 PDF	$m_t^{\text{out}} \pm \delta m_t^{\text{out}}$ [GeV]	Averaged $\chi^2/\text{d.o.f.}$	Probability $p\text{-value}$	$m_t^{\text{in}} - m_t^{\text{out}}$ [GeV]
<i>31 bins</i>				
<i>Full, <math>\mu_0 = H_T/2</math></i>	$173.38 \pm 1.34$	1.04	0.40 (0.8 $\sigma$ )	-0.18
<i>Full, <math>\mu_0 = E_T/2</math></i>	$172.84 \pm 1.33$	1.05	0.39 (0.9 $\sigma$ )	+0.36
<i>Full, <math>\mu_0 = m_t</math></i>	$174.11 \pm 1.39$	1.07	0.37 (0.9 $\sigma$ )	-0.91
<i>NWA, <math>\mu_0 = m_t</math></i>	$175.70 \pm 0.96$	1.17	0.24 (1.2 $\sigma$ )	-2.50
<i>NWA<sub>Prod.</sub>, <math>\mu_0 = m_t</math></i>	$169.93 \pm 0.98$	1.20	0.20 (1.3 $\sigma$ )	+3.27
<i>5 bins</i>				
<i>Full, <math>\mu_0 = H_T/2</math></i>	$173.15 \pm 1.32$	0.93	0.44 (0.8 $\sigma$ )	+0.05
<i>Full, <math>\mu_0 = E_T/2</math></i>	$172.55 \pm 1.18$	1.07	0.37 (0.9 $\sigma$ )	+0.65
<i>Full, <math>\mu_0 = m_t</math></i>	$173.92 \pm 1.38$	1.48	0.20 (1.3 $\sigma$ )	-0.72
<i>NWA, <math>\mu_0 = m_t</math></i>	$175.54 \pm 0.97$	1.38	0.24 (1.2 $\sigma$ )	-2.34
<i>NWA<sub>Prod.</sub>, <math>\mu_0 = m_t</math></i>	$169.37 \pm 1.43$	1.16	0.33 (1.0 $\sigma$ )	+3.83

# Modelling at hadron colliders

- Output of a measurement using Monte Carlo event generators is function of the pole mass



$$m_t^{\text{MC}} = m_t^{\text{pole}} + \Delta_m^{\text{pert}} + \Delta_m^{\text{non-pert}} + \Delta_m^{\text{MC}}$$

pQCD contribution:

- Perturbative correction
- Depends on MC parton shower setup

Non-perturbative contribution:

- Effects of hadronization model
- May depend on parton shower setup

Monte Carlo shift:

- Contribution arising from systematic MC uncertainties
- E.g. color reconnection, b-jet modeling, finite width, ...
- Should be covered by 'MC uncertainty' or better negligible

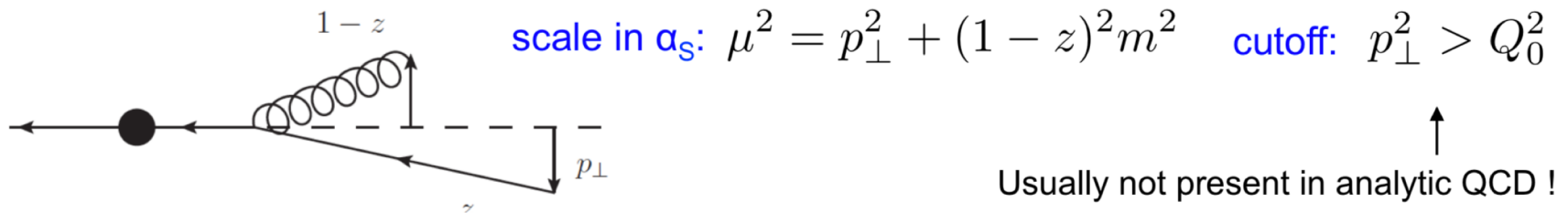
- Study the effects by comparison of an event generator and analytic QCD predictions in a controlled environment
- For example lepton collider in boosted topologies

Hoang et al. (ongoing)

# Modelling at hadron colliders

- One source of shifts may be due to radiation cutoffs

→ Coherent branching: (basis of the Herwig parton shower) Catani, Marchesini, Webber 1991  
Gieseke, Stephens, Webber, 2003



$$m_t^{\text{CB}}(Q_0) = m_t^{\text{pole}} - \frac{2}{3} Q_0 \alpha_s(Q_0) + \mathcal{O}(\alpha_s(Q_0)^2)$$

“Coherent-branching mass” is here the “Monte Carlo mass”

Herwig 7:  $Q_0 = 1.25 \text{ GeV} \rightarrow m_t^{\text{Herwig}} = m_t^{\text{CB}}(1.25 \text{ GeV})$

Hoang, Plätzer, Samitz `18

# Modelling at hadron colliders

- Unanswered question: does this effect persist if matching after decay ?
- Further restrictions of the analysis
  - Boosted top quarks
  - Narrow width approximation
  - Top production (2-jettiness)
- Needed to remove the restrictions
  - Parton shower algorithm for slow tops
  - Parton shower for unstable top quark
  - Factorized predictions including top decay

# Conclusions

- Direct measurements of the top-quark mass **can** be interpreted in terms of the pole mass
- While not necessary at present, it is possible to directly determine a short distance mass
  - This is **easy** for specific observables by re-expanding theory predictions in the on-shell scheme in terms of a different mass parameter
  - This is **difficult** using parton showers, since the underlying differential fixed-order prediction is given in function of the on-shell mass
- Ambiguities of parton shower modelling **may** and **should** be studied further